Vietnam Journal of Mechanics, VAST, Vol. 40, No. 1 (2018), pp. 89 – 103
DOI:10.15625/0866-7136/10579

STATIC AND FREE VIBRATION ANALYSES OF LAMINATED COMPOSITE SHELLS BY CELL-BASED SMOOTHED DISCRETE SHEAR GAP METHOD (CS-DSG3) USING THREE-NODE TRIANGULAR ELEMENTS

Pham Quoc Hoa[1,2], Tran The Van[2], Pham Tien Dat[1], Dang Trung Hau[3], Nguyen Viet Ha[1], Nguyen Manh Hung[2], Nguyen Thoi Trung[3,*]
[1] *Le Quy Don University, Hanoi, Vietnam*
[2] *Tran Dai Nghia University, Ho Chi Minh City, Vietnam*
[3] *Ton Duc Thang University, Ho Chi Minh City, Vietnam*
[*] E-mail: nguyenthoitrung@tdt.edu.vn
Received July 30, 2017

Abstract. A cell-based smoothed discrete shear gap method (CS-DSG3) using three-node triangular elements was recently proposed to improve the performance of the discrete shear gap method (DSG3) for static and free vibration analyses of isotropic Reissner-Mindlin plates and shells. In this paper, the CS-DSG3 is further extended for static and free vibration analyses of laminated composite shells. In the present method, the first-order shear deformation theory (FSDT) is used in the formulation due to the simplicity and computational efficiency. The accuracy and reliability of the proposed method are verified by comparing its numerical solutions with those of others available numerical results.

Keywords: Smoothed finite element methods (S-FEM), cell-based smoothed discrete shear gap method (CS-DSG3), laminated composite shell, first-order shear deformation theory (FSDT).

1. INTRODUCTION

Owning many superior properties as high strength-to-weight and high stiffness-to-weight ratios, excellent fatigue strength, etc., composite materials have been widely used in plate and shell structures in many engineering fields such as naval, automotive, aerospace, defense industries and many other areas. Many methods for analysis of the laminated composite plate and shell have been developed recently. For example, A. Bhimaraddi has proposed a three-dimensional (3D) elasticity solution for static and vibration of double curved shallow shell made of composite material [1, 2]. In this study, the shell thickness is divided into layers of smaller thickness, which can help increase the accuracy in analysis of thickness shell. However, the computational cost for 3D analysis is still much higher than that for two-dimensional (2D) analysis. Therefore, a 2D model was preferred for analysis of the laminated composite shell and attracted the concern of many researchers. For example, K. P. Rao [3] developed a rectangular laminated shell element. In these papers, the authors only used the classical laminated theory (CLT) which completed neglect the shear deformation effect, and hence had a negative influence to the accuracy of analysis results of thickness shell. To overcome the drawbacks, the first order shear deformation theory (FSDT) was used to analyze for the laminated shell. J. N. Reddy [4] presented a development of exact solutions based on the Sander shell theory for the double curved shell. S. J. Hossain et al. [5] developed a four node quadrilateral isoparametric element using mixed interpolation of tensorial components (MITC) approach. D. Chakravorty et al. [6] proposed an eight node curved quadrilateral isoparametric element for the vibration analysis of double curved laminated composite shells. The FSDT, however, the accuracy of solutions strongly depends on shear correction factors to ensure the stability of the solution [7]. Hence, the higher order shear deformation (HSDT), layerwise (LWT) or zigzag (ZIGT) theories have been proposed to analyze the laminated composite shell. For instance, L. Librescu and A. A. Khdeir [8,9] used the state space concept conjunction of the Lévy method for static and free vibration analyses of the laminated composite shell. J. N. Reddy and C. F. Liu [10] developed a HSDT for the laminated composite shell. In this study, the Navier-type exact solutions for static and free vibration analyses were presented for spherical and cylindrical shells. R. K. Khare et al. [11] presented a 2D HSDT for analysis of laminated composite and sandwich shallow shells subjected to thermal and mechanical loads. To achieve more accurate results for laminated shell, M. Y. Yasin [12] proposed a four-node quadrilateral element for static and free vibration analyses of laminated shallow shells based on the ZIGT. G. Giunta et al. [13] mixed the HSDT with LWT and ZIGT for analysis of the laminated double curved shell. A. J. M. Ferreira et al. [14] studied the radial basis functions (RBFs) collocation based on a LWT for the static and free vibration analyses of the laminated shells. From above literature review, it is obvious that, HSDT, LWT and ZIGT have been achieved the great interest from researchers. However, they have a limitation in computational cost which causes the limit of their practical applications. In addition, in recent years, many promising computational approaches have also been proposed for analyzing plate/shell problems. For example, Chien H. Thai et al. [15–17] developed isogeometric analysis for static, free vibration, and buckling analysis of laminated composite plates. T. Rabczuk et al. [18,19] used meshfree method based on the Kirchhoff–Love (KL) theory to investigate for crack and fluid-structure interaction of thin shells. N. Nguyen-Thanh et al. [20, 21] presented isogeometric analysis to study for thin shell structures.

On the other hand, in front of the development of numerical methods, Liu and Nguyen-Thoi [22] integrated the strain smoothing technique into the finite element method to create a series of smoothed finite element methods (S-FEM) including the cell-based smoothed finite element (CS-FEM) [23–28], the node-based smoothed finite element (NS-FEM) [29–31], the edge-based smooth finite element method (ES-FEM) [32,33], and the face-based smoothed finite element (FS-FEM) [34]. Each of these smoothed finite element methods has different properties and has been used to produce desired solutions for a wide class of benchmark and practical mechanics problems. The smoothed finite element methods have also been further investigated and applied to various problems as plates and shells [35–43], and some other applications.

Among the S-FEM models, the CS-FEM has shown some interesting properties in the solid mechanics problems. Extending the idea of the CS-FEM to plate structures, Nguyen-Thoi et al. [43] have recently formulated a cell-based smoothed stabilized discrete shear gap element (CS-DSG3) for static and free vibration analyses of isotropic shell structures by combining the CS-FEM with the original DSG3 [44]. In the CS-DSG3, each three-node triangular element will be divided into three sub-triangles, and in each sub-triangle, the stabilized DSG3 is used to compute the strains. Following that the strain smoothing technique on whole triangular element is used to smooth the strains on three sub-triangles. The numerical results have shown that the CS-DSG3 is free of shear locking and achieves a high accuracy compared with the exact solutions and other existing elements in the literature.

This paper aims to extend further the CS-DSG3 to static and free vibration analyses of the laminate composite shell. The FSDT and flat shell theory are used in the formulation due to the simplicity and computational efficiency. The accuracy and reliability of the proposed method are verified by comparing its numerical solutions with those of others available numerical results.

2. WEAK FORM OF LAMINATED COMPOSITE SHELL

A shell is a 3D structure and it is often convenient to define the geometry of shell structures in the global coordinate system. Based on the theories of formulation [45], shell elements can be classified into three main groups: (1) degenerated shell elements derived from the 3D solid theory; (2) curved shell elements based on general shell theory; and (3) flat shell elements formulated by combining a plane elastic membrane elements (plane stress elements) and a plate bending elements. Among these three groups, the flat shell elements are more popular due to simple formulation and low computational cost, and hence the theory of flat shell elements will be chosen to consider in this study.

To generate the element stiffness matrix for the membrane and plate bending elements, the elements must be defined in a local plane. Thus it is necessary to use local coordinates for computing the element mass, stiffness matrices and load vectors of the flat shell elements. In this case, a transformation between global and local coordinates is required and can be defined by using direction cosines. Based on the FSDT and flat shell theory, the standard weak-form Galerkin of shell problem is defined by

$$\int_{\Omega} \delta \mathbf{u}^T \mathbf{m} \ddot{\mathbf{u}} \mathrm{d}\Omega + \int_{\Omega} \delta \begin{bmatrix} \boldsymbol{\varepsilon}_m^T \\ \boldsymbol{\kappa}^T \\ \boldsymbol{\gamma}^T \end{bmatrix}^T \begin{bmatrix} \mathbf{D}_m & \mathbf{D}_{mb} & 0 \\ \mathbf{D}_{mb} & \mathbf{D}_b & 0 \\ 0 & 0 & \mathbf{D}_s \end{bmatrix} \begin{bmatrix} \boldsymbol{\varepsilon}_m \\ \boldsymbol{\kappa} \\ \boldsymbol{\gamma} \end{bmatrix} \mathrm{d}\Omega = \int_{\Omega} \delta \mathbf{u}^T \mathbf{b} \mathrm{d}\Omega, \qquad (1)$$

where $\mathbf{u} = \left\{ u_0, v_0, w_0, \beta_x, \beta_y, \beta_z \right\}^T$ is the displacement field at any point on the middle plane of shell with u_0, v_0, w_0 and $\beta_x, \beta_y, \beta_z$ denote the displacement components in the

x, y, z directions, respectively; $\mathbf{b}$ is an applied load vector; $\boldsymbol{\varepsilon}_m, \boldsymbol{\kappa}$ and $\boldsymbol{\gamma}$ are defined by

$$\boldsymbol{\varepsilon}_m = \{u_{0,x} \;\; v_{0,y} \;\; u_{0,y} + v_{0,x}\}^T, \boldsymbol{\kappa} = \{\beta_{x,x} \;\; \beta_{y,y} \;\; \beta_{x,y} + \beta_{y,x}\}^T, \boldsymbol{\gamma} = \{w_{0,x} + \beta_x \;\; w_{0,y} + \beta_y\}^T. \tag{2}$$

In Eq. (1), $\mathbf{D}_m$, $\mathbf{D}_b$, $\mathbf{D}_{mb}$ and $\mathbf{D}_s$ are the extensional, bending, bending-extension coupling stiffness, respectively, which are given by

$$\begin{aligned} (\mathbf{D}_m, \mathbf{D}_{mb}, \mathbf{D}_b) &= \int_{-h/2}^{h/2} (1, z, z^2)\overline{Q}_{ij} \mathrm{d}z, \quad (i, j = 1, 2, 6) \\ \mathbf{D}_s &= \int_{-h/2}^{h/2} \kappa \overline{Q}_{ij} \mathrm{d}z, \quad (i, j = 4, 5) \end{aligned} \tag{3}$$

where h is the thickness of the shell; $\kappa = 5/6$ is shear coefficient; $\overline{Q}_{ij}$ are the transformed material constants of the k^{th} lamina [7]; $\mathbf{m}$ is the mass matrix containing the mass density of the material ρ, expressed by

$$\mathbf{m} = \sum_{k=1}^{N} \rho^k \int_{z_k}^{z_{k+1}} \begin{bmatrix} 1 & 0 & 0 & z & 0 & 0 \\ 0 & 1 & 0 & 0 & z & 0 \\ 0 & 0 & 1 & 0 & 0 & 0 \\ z & 0 & 0 & z^2 & 0 & 0 \\ 0 & z & 0 & 0 & z^2 & 0 \\ 0 & 0 & 0 & 0 & 0 & 0 \end{bmatrix} \mathrm{d}z. \tag{4}$$

3. CS-DSG3 FORMULATION FOR LAMINATED COMPOSITE SHELL

In the DSG3 [44], the shear strain is linear interpolated based on the concept "shear gap" of displacement along the sides of the elements by using the standard element shape functions. Accordingly, the approximation $\mathbf{u}_e$ of a 3-node triangular shell element Ω_e can be written as

$$\mathbf{u}_e = \sum_{I=1}^{3} N_I(\mathbf{x}) \mathbf{I}_6 \mathbf{d}_{eI} = \sum_{I=1}^{3} \mathbf{N}_I \mathbf{d}_{eI}, \tag{5}$$

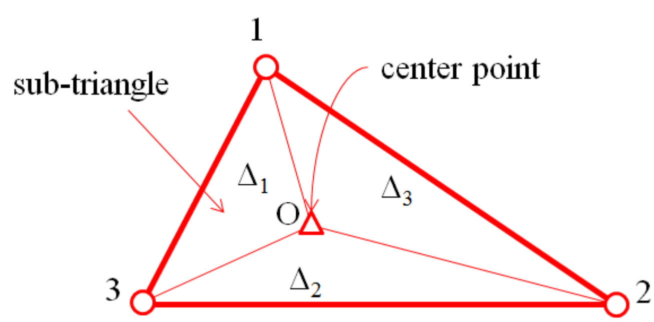

Fig. 1. Three sub-triangles created from the triangle 1-2-3 in CS-DSG3 by connecting the central point O with three field nodes 1, 2 and 3

where $\mathbf{d}_{eI} = \{u_I, v_I, w_I, \beta_{xI}, \beta_{yI}, \beta_{zI}\}^T$ is the nodal degrees of freedom associated with the Ith node and $N_I(\mathbf{x})$ is linear shape functions in a natural coordinate defined by

$$N_1 = 1 - \xi - \eta; \quad N_2 = \xi; \quad N_3 = \eta. \tag{6}$$

Then, the membrane, bending and shear strains in the element are then obtained by

$$\begin{aligned} \boldsymbol{\varepsilon}_m &= [\mathbf{B}_{m1}, \mathbf{B}_{m2}, \mathbf{B}_{m3}]\, \mathbf{d}_e = \mathbf{B}_m \mathbf{d}_e, \\ \boldsymbol{\kappa} &= [\mathbf{B}_{b1}, \mathbf{B}_{b2}, \mathbf{B}_{b3}]\, \mathbf{d}_e = \mathbf{B}_b \mathbf{d}_e, \\ \boldsymbol{\gamma} &= [\mathbf{B}_{s1}, \mathbf{B}_{s2}, \mathbf{B}_{s3}]\, \mathbf{d}_e = \mathbf{B}_s \mathbf{d}_e, \end{aligned} \tag{7}$$

where $\mathbf{B}_{mi}$, $\mathbf{B}_{bi}$ and $\mathbf{B}_{si}$ are determined as $\mathbf{R}_i$, $\mathbf{B}_i$ and $\mathbf{S}_i$ in [43].

The global stiffness matrix now can be written by

$$\mathbf{K}^{DSG3} = \sum_{e=1}^{N_n} \mathbf{K}_e^{DSG3}, \tag{8}$$

where $\mathbf{K}_e^{DSG3}$ is the element stiffness matrix of the DSG3 element and is given by

$$\mathbf{K}_e^{DSG3} = \mathbf{T}^T \left(\int_{\Omega_e} \begin{Bmatrix} \mathbf{B}_m \\ \mathbf{B}_b \\ \mathbf{B}_s \end{Bmatrix}^T \begin{bmatrix} \mathbf{D}_m & \mathbf{D}_{mb} & \mathbf{0} \\ \mathbf{D}_{mb} & \mathbf{D}_b & \mathbf{0} \\ \mathbf{0} & \mathbf{0} & \mathbf{D}_s \end{bmatrix} \begin{Bmatrix} \mathbf{B}_m \\ \mathbf{B}_b \\ \mathbf{B}_s \end{Bmatrix} \mathrm{d}\Omega \right) \mathbf{T}, \tag{9}$$

in which $\mathbf{T}$ is the transformation matrix for whole element that is defined by

$$\mathbf{T} = \mathrm{diag}(\mathbf{T}_0, \mathbf{T}_0, \mathbf{T}_0), \tag{10}$$

and $\mathbf{T}$ is a transformation matrix at each point [45].

In the CS-DSG3, each triangular element was divided into three sub-triangles, Δ_j, by connecting the central point of the element to three field nodes as shown in Fig. 1. Then the displacement vector at central point was assumed to be the simple average of three displacement vectors of three field nodes. To avoid the shear locking phenomenon, in each sub-triangles, the stabilized DSG3 was used to compute the strain fields. The detail formulation of CS-DSG3 can be found in references [43,46].

The smoothed membrane, bending and shear strains in the CS-DSG3 are expressed by

$$\boldsymbol{\varepsilon}_m = \widetilde{\mathbf{B}}_m \mathbf{T} \mathbf{d}_e, \quad \boldsymbol{\kappa} = \widetilde{\mathbf{B}}_b \mathbf{T} \mathbf{d}_e, \quad \boldsymbol{\gamma} = \widetilde{\mathbf{B}}_s \mathbf{T} \mathbf{d}_e, \tag{11}$$

where $\widetilde{\mathbf{B}}_m$, $\widetilde{\mathbf{B}}_b$ and $\widetilde{\mathbf{B}}_s$ are, respectively, the smoothed membrane, bending and shear gradient matrices expressed by

$$\widetilde{\mathbf{B}}_k = \frac{1}{A_e} \sum_{i=1}^{3} A_{\Delta_i} \mathbf{B}_k^{\Delta_i}, \quad k = m, b, s \tag{12}$$

where A_e and A_{Δ_i} are the area of element and sub-triangle Δ_i, respectively; $\mathbf{B}_m^{\Delta_j}, \mathbf{B}_b^{\Delta_j}, \mathbf{B}_s^{\Delta_j}$ ($j = 1, 2, 3$) are computed similarly as the matrices $\mathbf{B}_m, \mathbf{B}_b, \mathbf{B}_s$ of the DSG3 in Eqs. (7), but with two following changes: 1) the coordinates of three node $\mathbf{x}_i = \begin{bmatrix} x_i & y_i \end{bmatrix}^T$, $i = 1, 2, 3$ are replaced by three nodes of sub-triangle Δ_j, respectively; and 2) the area A_e is replaced by the area A_{Δ_j} of sub-triangle Δ_j. These computational details can be found in [43] By substituting Eq. (11) into Eq. (1), the equilibrium equation for the laminated shell is now expressed in the form of

$$\mathbf{M}\ddot{\mathbf{d}} + \mathbf{K}\mathbf{d} = \mathbf{F}, \tag{13}$$

in which **M** and **K** are the global mass and stiffness matrices, **F** is the global load vector. They are obtained by assembling from local matrices and expressed as follows

$$\mathbf{M} = \sum_{e=1}^{N_e} \mathbf{M}_e = \sum_{e=1}^{N_e} \int_{\Omega_e} \mathbf{T}^T \mathbf{N}^T \mathbf{m} \mathbf{N} \mathbf{T} \mathrm{d}\Omega, \tag{14}$$

$$\mathbf{K} = \sum_{e=1}^{N_e} \mathbf{K}_e^{\mathrm{CS-DSG3}} = \sum_{e=1}^{N_e} \int_{\Omega_e} \mathbf{T}^T \left\{ \widetilde{\mathbf{B}}_m^T \quad \widetilde{\mathbf{B}}_b^T \quad \widetilde{\mathbf{B}}_s^T \right\} \begin{bmatrix} \mathbf{D}_m & \mathbf{D}_{mb} & 0 \\ \mathbf{D}_{mb} & \mathbf{D}_b & 0 \\ 0 & 0 & \mathbf{D}_s \end{bmatrix} \begin{Bmatrix} \widetilde{\mathbf{B}}_m^T \\ \widetilde{\mathbf{B}}_b^T \\ \widetilde{\mathbf{B}}_s^T \end{Bmatrix} \mathbf{T} \mathrm{d}\Omega, \tag{15}$$

$$\mathbf{F} = \sum_{e=1}^{N_e} \mathbf{F}_e = \sum_{e=1}^{N_e} \int_{\Omega_e} \mathbf{T}^T \mathbf{N}^T \mathbf{b} \mathrm{d}\Omega, \tag{16}$$

From Eq. (2), we can see the independence between the strain components and the drilling degree of freedom, β_z. This is the cause of singularity in the global stiffness matrix when all the elements meeting at node are coplanar and there is no coupling between the membrane stiffness and bending stiffness of the element. To deal this problem, the null values of the stiffness matrix corresponding to β_z are replaced by approximate values. This approximate value is taken to be equal to 10^{-3} times the maximum diagonal value in the element stiffness matrix [43].

Note that while the accuracy of the CS-DSG3 [46] and that of the ES-DSG3 [39] are almost the same [46], the CS-DSG3 has lower computational cost. It is because the CS-DSG3 only requires the local computation located inside the element which is much more convenient than the ES-DSG3. This advantage of the CS-DSG3 is even further promoted for shell elements

4. NUMERICAL RESULTS

In this section, the static and free-vibration analyses of laminated composite spherical and cylindrical shells as shown in Fig. 2 are conducted using the proposed method CS-DSG3. In static analysis, these shells are assumed to be subjected to uniform distributed, sinusoidal and concentrated loads. The effects of the boundary conditions, length to radius ratio and fiber direction on behavior of these shells are considered. The obtained results are compared to the other existing numerical solutions to show the accuracy and stability of the CS-DSG3 in laminated shell analyses. For the convenient comparison, the non-dimensional central deflection and natural frequencies are introduced by

$$\overline{w} = \frac{1000w\left(a/2, b/2, 0\right) t^3 E_2}{Pa^4}, \quad \overline{\omega} = \omega \left(a^2/h\right) \sqrt{\rho/E^2}. \tag{17}$$

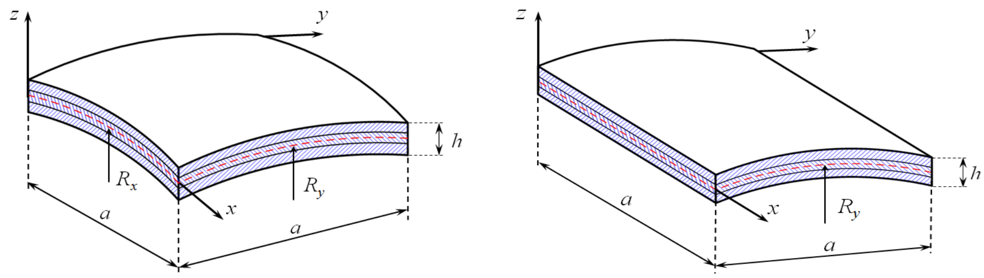

(a) Spherical shell model ($R_x = R_y = R$) (b) Cylindrical shell model ($R_x = \infty, R_y = R$)

Fig. 2. Geometry for laminated composite shells

4.1. Static analysis

4.1.1. *Laminated spherical shell*

Firstly, the static analysis of a simply supported laminated spherical shell is studied. The shell composes of several layers such as [0°/90°], [0°/90°/0°], [0°/90°/90°/0°]. All the plies have the same thickness and material with mechanical properties given by: $E_1 = 25E_2$, $G_{12} = 0.5E_2$, $G_{13} = 0.5E_2$, $G_{23} = 0.2E_2$, $v_{12} = 0.25$. Tab. 1 presents the non-dimensional central deflections of the laminated shell subjected to sinusoidal loading, by the CS-DSG3 in comparison with those by the DSG3 [44] and Reddy and Liu [10] using the FSDT. Further, the non-dimensional central displacements of laminated shell under

Table 1. The non-dimensional center deflections of the laminated spherical shells under sinusoidal load

R/a	Theory	0°/90°		0°/90°/0°		0°/90°/90°/0°	
		$a/h=10$	$a/h=100$	$a/h=10$	$a/h=100$	$a/h=10$	$a/h=100$
5	Reddy and Liu FSDT [10]	11.4290	1.1948	6.4253	1.0337	6.3623	1.0279
	DSG3 (24×24)	11.2516	1.1630	6.3442	1.0087	6.2653	1.0024
	CS-DSG3 (8×8)	10.7714	1.1287	6.1245	0.9772	6.0546	0.9713
	CS-DSG3 (12×12)	11.1020	1.1527	6.2837	0.9999	6.2135	0.9940
	CS-DSG3 (24×24)	11.3055	1.1645	6.3672	1.0113	6.2969	1.0053
10	Reddy and Liu FSDT [10]	12.1230	3.5760	6.6247	2.4109	6.5595	2.4030
	DSG3 (24×24)	12.0923	3.5495	6.6487	2.4103	6.5701	2.4009
	CS-DSG3 (8×8)	11.5641	3.4124	6.3912	2.0314	6.3294	2.2933
	CS-DSG3 (12×12)	11.9266	3.5118	6.5584	2.3729	6.4861	2.3649
	CS-DSG3 (24×24)	12.1165	3.5625	6.6612	2.4123	6.5886	2.4041
100	Reddy and Liu FSDT [10]	12.3700	10.446	6.6923	4.3026	6.6264	4.3021
	DSG3 (24×24)	12.3911	10.465	6.7438	4.3438	6.6640	4.3391
	CS-DSG3 (8×8)	11.8434	9.7343	6.4817	4.0756	6.4092	4.0730
	CS-DSG3 (12×12)	12.2177	10.277	6.6518	4.2516	6.5786	4.2507
	CS-DSG3 (24×24)	12.4478	10.522	6.7564	4.3453	6.6828	4.3447

uniformly distributed and point load obtained by the CS-DSG3 are listed in Tabs. 2 and 3 along with those by Reddy and Liu [10] using the FSDT, respectively. The various ratios of values side-to-thickness and values of radius-to-thickness are also examined. It is seen that the results by the CS-DSG3 are softer than those of the DSG3 and agree well with those published by Reddy and Liu [10] using the FSDT.

Table 2. The non-dimensional center deflections of the laminated spherical shells under uniform load

R/a	Theory	$0°/90°$		$0°/90°/0°$		$0°/90°/90°/0°$	
		$a/h=10$	$a/h=100$	$a/h=10$	$a/h=100$	$a/h=10$	$a/h=100$
5	Reddy and Liu FSDT [10]	19.9440	1.7535	9.7937	1.5118	9.8249	1.5358
	CS-DSG3 (8×8)	16.8807	1.6712	9.3469	1.4427	9.3365	1.4630
	CS-DSG3 (12×12)	17.3799	1.6926	9.5609	1.4628	9.5678	1.4856
	CS-DSG3 (24×24)	17.6854	1.7059	9.6914	1.4762	9.7095	1.4995
10	Reddy and Liu FSDT [10]	19.0650	5.5428	10.110	3.6445	10.141	3.7208
	CS-DSG3 (8×8)	18.2055	5.3245	9.7984	3.5237	9.7879	3.5780
	CS-DSG3 (12×12)	18.7586	5.4562	10.025	3.6008	10.032	3.6713
	CS-DSG3 (24×24)	19.0971	5.5213	10.164	3.6454	10.186	3.7221
100	Reddy and Liu FSDT [10]	19.4640	16.6450	10.2180	6.6421	10.2490	6.6772
	CS-DSG3 (8×8)	18.6726	15.5468	9.95190	6.3613	9.94110	6.4508
	CS-DSG3 (12×12)	19.2457	16.3981	10.1839	6.5904	10.1908	6.7124
	CS-DSG3 (24×24)	19.5964	16.7744	10.3253	6.7133	10.3436	6.8493

Table 3. The non-dimensional center deflections of the laminated spherical shells under central concentrated load

R/a	Theory	$0°/90°$		$0°/90°/0°$		$0°/90°/90°/0°$	
		$a/h=10$	$a/h=100$	$a/h=10$	$a/h=100$	$a/h=10$	$a/h=100$
5	Reddy and Liu FSDT [10]	71.015	-	51.410	-	49.360	-
	CS-DSG3 (8×8)	57.019	6.7337	38.123	5.8155	36.595	5.3842
	CS-DSG3 (12×12)	60.573	7.3182	41.223	6.2661	39.461	5.7427
	CS-DSG3 (24×24)	65.315	7.8136	45.653	6.6565	43.682	6.0465
10	Reddy and Liu FSDT [10]	73.836	-	52.273	-	50.186	-
	CS-DSG3 (8×8)	60.590	16.625	39.479	11.927	37.906	11.122
	CS-DSG3 (12×12)	64.279	17.456	42.636	12.645	40.823	11.652
	CS-DSG3 (24×24)	69.145	18.078	47.133	13.176	45.109	12.049
100	Reddy and Liu FSDT [10]	74.940	-	52.666	-	50.565	-
	CS-DSG3 (8×8)	61.833	43.141	39.930	19.481	38.345	18.515
	CS-DSG3 (12×12)	65.578	45.176	43.109	20.727	41.281	19.438
	CS-DSG3 (24×24)	70.489	46.333	47.624	21.504	45.589	20.020

4.1.2. *Laminated cylindrical shell*

Next, the static analysis of the laminated cylindrical shells is considered. All of the layers are made by the same material with mechanical properties given by: $E_1 = 19.2\times10^6$ Psi; $E_2 = 1.56\times10^6$ Psi, $G_{12} = G_{13} = 0.82\times10^6$ Psi, $G_{23} = 0.523\times10^6$ Psi, $v_{12} = 0.24$. The shell is subjected to a sinusoidal distributed load. Tab. 4 presents the non-dimensional center deflections of the shell in comparison with those published by Khdeir et al. [9]. Despite using a coarse mesh (12×12), it is observed that the obtained results match well with exact solution by Khdeir et al. [9].

Table 4. The non-dimensional center deflections of the laminated cylindrical shells under sinusoidal distributed load

R/a ($a/h = 10$)	Theory	$0°/90°$	$0°/90°/0°$	$0°/90°/90°/0°$
5	FSDT [9]	1.5614	0.8999	-
	CS-DSG3 (8×8)	1.4780	0.9090	0.8993
	CS-DSG3 (12×12)	1.5261	0.9359	0.9261
	CS-DSG3 (24×24)	1.5555	0.9525	0.9426
10	FSDT [9]	1.5910	0.9434	-
	CS-DSG3 (8×8)	1.5257	0.9269	0.9175
	CS-DSG3 (12×12)	1.5756	0.9545	0.9450
	CS-DSG3 (24×24)	1.6062	0.9714	0.9618
50	FSDT [9]	1.6000	0.9583	-
	CS-DSG3 (8×8)	1.5420	0.9327	0.9234
	CS-DSG3 (12×12)	1.5926	0.9605	0.9511
	CS-DSG3 (24×24)	1.6235	0.9776	0.9681

4.2. Free vibration analysis

In this example, the free vibration analysis of simply supported laminated composite spherical and cylindrical shells is considered. All layers of these shells are assumed to be of the same thickness and material with mechanical properties given by: $E_1 = 25E_2$, $G_{12} = 0.5E_2$, $G_{13} = 0.5E_2$, $G_{23} = 0.2E_2$, $v_{12} = 0.25$. The non-dimensional frequencies of the laminated spherical shell by the CS-DSG3 are compared with those by Reddy and Liu [10] in Tab. 5. Tab. 6 contains non-dimensional frequencies of the laminated cylindrical shell which are compared with analytical solutions by Reddy and Liu [10]. The shape of the first-six mode shapes of these shells by the CS-DSG3 is also displayed in Figs. 3 and 4. It can be seen that the results obtained by the CS-DSG3 agree well with reference solutions using FSDT of Reddy and Liu [10].

Table 5. Non-dimensional frequencies $\overline{\omega}$ of a cross-ply laminated spherical shells ($R_x = R_y = R$)

R/a	Theory	$0^\circ/90^\circ$		$0^\circ/90^\circ/0^\circ$		$0^\circ/90^\circ/90^\circ/0^\circ$	
		$a/h=10$	$a/h=100$	$a/h=10$	$a/h=100$	$a/h=10$	$a/h=100$
5	FSDT [10]	9.2309	28.8250	12.3720	30.9930	12.4370	12.3800
	CS-DSG3 (8×8)	9.6105	30.0054	12.7958	32.2573	12.8746	32.3533
	CS-DSG3 (12×12)	9.3569	29.3434	12.4863	31.5120	12.5614	31.6050
	CS-DSG3 (24×24)	9.2078	28.9614	12.3037	31.0822	12.3766	31.1728
10	FSDT [10]	8.9841	16.7060	12.2150	20.3470	12.4370	20.3800
	CS-DSG3 (8×8)	9.3713	17.4354	12.6673	21.2329	12.7437	21.2675
	CS-DSG3 (12×12)	9.1206	16.9796	12.3583	20.6578	12.4314	20.6921
	CS-DSG3 (24×24)	8.9734	16.7380	12.1762	20.3421	12.2474	20.3764
100	FSDT [10]	8.9009	9.7896	12.1630	15.2440	12.2280	15.2450
	CS-DSG3 (8×8)	9.2911	10.358	12.6241	16.0094	12.6998	16.0110
	CS-DSG3 (12×12)	9.0412	9.9574	12.3152	15.4827	12.3878	15.4837
	CS-DSG3 (24×24)	8.8946	9.7703	12.1333	15.2047	12.2040	15.2057

Table 6. The non-dimensional $\overline{\omega}$ frequencies of a cross-ply laminated cylindrical shells ($R_y = R, R_x = \infty$)

R/a	Theory	$0^\circ/90^\circ$		$0^\circ/90^\circ/0^\circ$		$0^\circ/90^\circ/90^\circ/0^\circ$	
		$a/h=10$	$a/h=100$	$a/h=10$	$a/h=100$	$a/h=10$	$a/h=100$
5	FSDT [10]	8.9082	16.6680	12.2070	20.332	12.2670	20.3610
	Present (8×8)	9.2805	17.1638	12.4794	20.9195	12.5887	20.9538
	Present (12×12)	9.0985	16.8699	12.2934	20.5549	12.3868	20.5866
	Present (24×24)	9.0123	16.7363	12.2064	20.3824	12.2883	20.4132
10	FSDT [10]	8.8879	11.831	12.1730	16.6250	12.2360	16.6340
	Present (8×8)	9.3048	12.4510	12.6379	17.4240	12.7141	17.4355
	Present (12×12)	9.0550	12.0455	12.3289	16.8880	12.4019	16.8991
	Present (24×24)	8.9084	11.8461	12.1468	16.6014	12.2180	16.6126
100	FSDT [10]	8.8974	9.7108	12.1630	15.1980	12.2270	15.1990
	Present (8×8)	9.2853	10.280	12.6222	15.9617	12.6969	15.9618
	Present (12×12)	9.0356	9.8801	12.3134	15.4353	12.3849	15.4348
	Present (24×24)	8.8891	9.6935	12.1315	15.1576	12.2011	15.1571

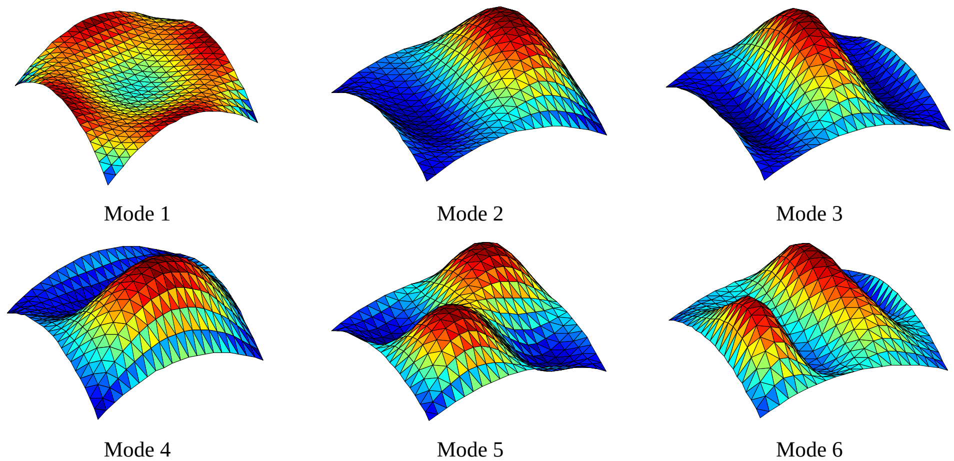

Fig. 3. The first six mode shapes of the laminated spherical shell by CS-DSG3 $(R/a = 10, a/h = 10, 0^\circ/90^\circ/0^\circ)$

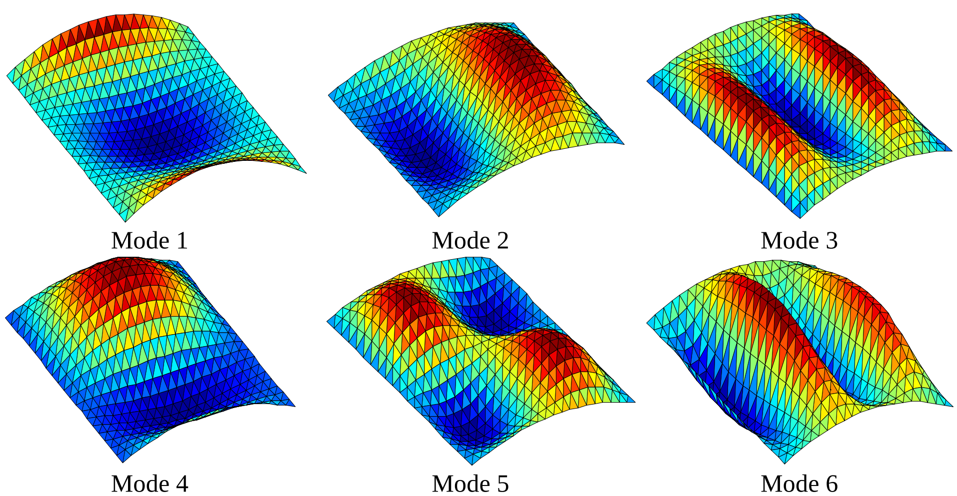

Fig. 4. The first six mode shapes of the laminated cylindrical shell by CS-DSG3 $(R/a = 10, a/h = 100, 0^\circ/90^\circ/0^\circ)$

5. CONCLUSIONS

The paper presents an extension of the CS-DSG3 using the FSDT for static and free vibration analyses of laminated composite shells. Through the present formulations and obtained numerical results, some main points can be withdrawn as:

i). The CS-DSG3 uses three-node triangular elements that are easier generated automatically for arbitrary complex geometrical domains.

ii). The CS-DSG3 uses only minimum degrees of freedom at each vertex node, so we can expect an efficient analysis in term of computational cost. The CS-DSG3 is free of shear locking for laminated composite shells.

iii). Due to using the gradient smoothing technique which can help soften the over-stiff behavior in the DSG3, the proposed CS-DSG3 improves significantly the accuracy of the numerical results and has a good convergence performance.

iv). The accuracy and reliability of the CS-DSG3 are verified by comparing its numerical solutions with those of other available numerical results. The results by the CS-DSG3 agree well with all reference solutions in different analyses.

The method presented herein is promising to be an effectively alternative method of classical finite elements for analysis of laminated composite shells in practice.

ACKNOWLEDGEMENTS

This research is funded by Vietnam National Foundation for Science and Technology Development (NAFOSTED) under grant number 107.02-2017.08.

REFERENCES

[1] A. Bhimaraddi. Free vibration analysis of doubly curved shallow shells on rectangular planform using three-dimensional elasticity theory. *International Journal of Solids and Structures*, **27**, (7), (1991), pp. 897–913. doi:10.1016/0020-7683(91)90023-9.

[2] A. Bhimaraddi. Three-dimensional elasticity solution for static response of orthotropic doubly curved shallow shells on rectangular planform. *Composite Structures*, **24**, (1), (1993), pp. 67–77. doi:10.1016/0263-8223(93)90056-v.

[3] K. P. Rao. A rectangular laminated anisotropic shallow thin shell finite element. *Computer Methods in Applied Mechanics and Engineering*, **15**, (1), (1978), pp. 13–33. doi:10.1016/0045-7825(78)90003-8.

[4] J. N. Reddy. Exact solutions of moderately thick laminated shells. *Journal of Engineering Mechanics*, **110**, (5), (1984), pp. 794–809. doi:10.1061/(asce)0733-9399(1984)110:5(794).

[5] S. J. Hossain, P. K. Sinha, and A. H. Sheikh. A finite element formulation for the analysis of laminated composite shells. *Computers & Structures*, **82**, (20-21), (2004), pp. 1623–1638. doi:10.1016/j.compstruc.2004.05.004.

[6] D. Chakravorty, J. N. Bandyopadhyay, and P. K. Sinha. Free vibration analysis of point-supported laminated composite doubly curved shells - A finite element approach. *Computers & Structures*, **54**, (2), (1995), pp. 191–198. doi:10.1016/0045-7949(94)00329-2.

[7] J. N. Reddy. *Mechanics of laminated composite plates and shells: Theory and analysis*. CRC Press, (2004).

[8] L. Librescu, A. A. Khdeir, and D. Frederick. A shear deformable theory of laminated composite shallow shell-type panels and their response analysis I: Free vibration and buckling. *Acta Mechanica*, **76**, (1-2), (1989), pp. 1–33. doi:10.1007/bf01175794.

[9] A. A. Khdeir, L. Librescu, and D. Frederick. A shear deformable theory of laminated composite shallow shell-type panels and their response analysis II: Static response. *Acta Mechanica*, **77**, (1-2), (1989), pp. 1–12. doi:10.1007/bf01379740.

[10] J. N. Reddy and C. F. Liu. A higher-order shear deformation theory of laminated elastic shells. *International Journal of Engineering Science*, **23**, (3), (1985), pp. 319–330. doi:10.1016/0020-7225(85)90051-5.

[11] R. K. Khare, T. Kant, and A. K. Garg. Closed-form thermo-mechanical solutions of higher-order theories of cross-ply laminated shallow shells. *Composite Structures*, **59**, (3), (2003), pp. 313–340. doi:10.1016/s0263-8223(02)00245-3.

[12] M. Y. Yasin and S. Kapuria. An efficient layerwise finite element for shallow composite and sandwich shells. *Composite Structures*, **98**, (2013), pp. 202–214. doi:10.1016/j.compstruct.2012.10.048.

[13] G. Giunta, F. Biscani, S. Belouettar, and E. Carrera. Hierarchical modelling of doubly curved laminated composite shells under distributed and localised loadings. *Composites Part B: Engineering*, **42**, (4), (2011), pp. 682–691. doi:10.1016/j.compositesb.2011.02.002.

[14] A. J. M. Ferreira, E. Carrera, M. Cinefra, and C. M. C. Roque. Analysis of laminated doubly-curved shells by a layerwise theory and radial basis functions collocation, accounting for through-the-thickness deformations. *Computational Mechanics*, **48**, (1), (2011), pp. 13–25. doi:10.1007/s00466-011-0579-4.

[15] C. H. Thai, H. Nguyen-Xuan, N. Nguyen-Thanh, T.-H. Le, T. Nguyen-Thoi, and T. Rabczuk. Static, free vibration, and buckling analysis of laminated composite Reissner–Mindlin plates using NURBS-based isogeometric approach. *International Journal for Numerical Methods in Engineering*, **91**, (6), (2012), pp. 571–603. doi:10.1002/nme.4282.

[16] C. H. Thai, A. J. M. Ferreira, S. P. A. Bordas, T. Rabczuk, and H. Nguyen-Xuan. Isogeometric analysis of laminated composite and sandwich plates using a new inverse trigonometric shear deformation theory. *European Journal of Mechanics-A/Solids*, **43**, (2014), pp. 89–108. doi:10.1016/j.euromechsol.2013.09.001.

[17] C. H. Thai, H. Nguyen-Xuan, S. P. A. Bordas, N. Nguyen-Thanh, and T. Rabczuk. Isogeometric analysis of laminated composite plates using the higher-order shear deformation theory. *Mechanics of Advanced Materials and Structures*, **22**, (6), (2015), pp. 451–469. doi:10.1080/15376494.2013.779050.

[18] T. Rabczuk, P. M. A. Areias, and T. Belytschko. A meshfree thin shell method for non-linear dynamic fracture. *International Journal for Numerical Methods in Engineering*, **72**, (5), (2007), pp. 524–548. doi:10.1002/nme.2013.

[19] T. Rabczuk, R. Gracie, J.-H. Song, and T. Belytschko. Immersed particle method for fluid-structure interaction. *International Journal for Numerical Methods in Engineering*, **81**, (1), (2010), pp. 48–71. doi:10.1002/nme.2670.

[20] N. Nguyen-Thanh, J. Kiendl, H. Nguyen-Xuan, R. Wüchner, K.-U. Bletzinger, Y. Bazilevs, and T. Rabczuk. Rotation free isogeometric thin shell analysis using PHT-splines. *Computer Methods in Applied Mechanics and Engineering*, **200**, (47-48), (2011), pp. 3410–3424. doi:10.1016/j.cma.2011.08.014.

[21] N. Nguyen-Thanh, N. Valizadeh, M. N. Nguyen, H. Nguyen-Xuan, X. Zhuang, P. Areias, G. Zi, Y. Bazilevs, L. De Lorenzis, and T. Rabczuk. An extended isogeometric thin shell analysis based on Kirchhoff–Love theory. *Computer Methods in Applied Mechanics and Engineering*, **284**, (2015), pp. 265–291. doi:10.1016/j.cma.2014.08.025.

[22] G. R. Liu and T. Nguyen-Thoi. *Smoothed finite element methods*. CRC Press, Taylor and Francis Group, NewYork, (2010).

[23] G. R. Liu, K. Y. Dai, and T. T. Nguyen. A smoothed finite element method for mechanics problems. *Computational Mechanics*, **39**, (6), (2007), pp. 859–877. doi:10.1007/s00466-006-0075-4.

[24] G. R. Liu, T. Nguyen-Thoi, H. Nguyen-Xuan, K. Y. Dai, and K. Y. Lam. On the essence and the evaluation of the shape functions for the smoothed finite element method (SFEM). *International Journal for Numerical Methods in Engineering*, **77**, (13), (2009), pp. 1863–1869. doi:10.1002/nme.2587.

[25] T. T. Nguyen, G. R. Liu, K. Y. Dai, and K. Y. Lam. Selective smoothed finite element method. *Tsinghua Science & Technology*, **12**, (5), (2007), pp. 497–508. doi:10.1016/s1007-0214(07)70125-6.

[26] G. R. Liu, H. Nguyen-Xuan, and T. Nguyen-Thoi. A theoretical study on the smoothed FEM (S-FEM) models: Properties, accuracy and convergence rates. *International Journal for Numerical Methods in Engineering*, **84**, (10), (2010), pp. 1222–1256. doi:10.1002/nme.2941.

[27] G. R. Liu, T. T. Nguyen, K. Y. Dai, and K. Y. Lam. Theoretical aspects of the smoothed finite element method (SFEM). *International Journal for Numerical Methods in Engineering*, **71**, (8), (2007), pp. 902–930. doi:10.1002/nme.1968.

[28] D. T. Hau, N. T. M. Hanh, and N. T. Trung. A cell-based smoothed discrete shear gap method (CS-FEM-DSG3) for dynamic response of laminated composite plate subjected to blast loading. *Vietnam Journal of Mechanics*, **37**, (2), (2015), pp. 81–90. doi:10.15625/0866-7136/37/2/5019.

[29] G. R. Liu, T. Nguyen-Thoi, H. Nguyen-Xuan, and K. Y. Lam. A node-based smoothed finite element method (NS-FEM) for upper bound solutions to solid mechanics problems. *Computers & Structures*, **87**, (1-2), (2009), pp. 14–26. doi:10.1016/j.compstruc.2008.09.003.

[30] T. Nguyen-Thoi, G. R. Liu, H. Nguyen-Xuan, and C. Nguyen-Tran. Adaptive analysis using the node-based smoothed finite element method (NS-FEM). *International Journal for Numerical Methods in Biomedical Engineering*, **27**, (2), (2011), pp. 198–218. doi:10.1002/cnm.1291.

[31] T. Nguyen-Thoi, G. R. Liu, and H. Nguyen-Xuan. Additional properties of the node-based smoothed finite element method (NS-FEM) for solid mechanics problems. *International Journal of Computational Methods*, **6**, (04), (2009), pp. 633–666. doi:10.1142/s0219876209001954.

[32] G. R. Liu, T. Nguyen-Thoi, and K. Y. Lam. An edge-based smoothed finite element method (ES-FEM) for static, free and forced vibration analyses of solids. *Journal of Sound and Vibration*, **320**, (4-5), (2009), pp. 1100–1130. doi:10.1016/j.jsv.2008.08.027.

[33] T. Nguyen-Thoi, G. R. Liu, and H. Nguyen-Xuan. An n-sided polygonal edge-based smoothed finite element method (nES-FEM) for solid mechanics. *International Journal for Numerical Methods in Biomedical Engineering*, **27**, (9), (2011), pp. 1446–1472. doi:10.1002/cnm.1375.

[34] T. Nguyen-Thoi, G. R. Liu, K. Y. Lam, and G. Y. Zhang. A face-based smoothed finite element method (FS-FEM) for 3D linear and geometrically non-linear solid mechanics problems using 4-node tetrahedral elements. *International journal for numerical methods in Engineering*, **78**, (3), (2009), pp. 324–353. doi:10.1002/nme.2491.

[35] T. Nguyen-Thoi, P. Phung-Van, H. Luong-Van, H. Nguyen-Van, and H. Nguyen-Xuan. A cell-based smoothed three-node Mindlin plate element (CS-MIN3) for static and free vibration analyses of plates. *Computational Mechanics*, **51**, (1), (2013), pp. 65–81. doi:10.1007/s00466-012-0705-y.

[36] X. Y. Cui, G. R. Liu, G. Y. Li, X. Zhao, T. Nguyen-Thoi, and G. Y. Sun. A smoothed finite element method (SFEM) for linear and geometrically nonlinear analysis of plates and shells. *Comput Model Eng Sci*, **28**, (2), (2008), pp. 109–125.

[37] C. H. Thai, L. V. Tran, D. T. Tran, T. Nguyen-Thoi, and H. Nguyen-Xuan. Analysis of laminated composite plates using higher-order shear deformation plate theory and node-based smoothed discrete shear gap method. *Applied Mathematical Modelling*, **36**, (11), (2012), pp. 5657–5677. doi:10.1016/j.apm.2012.01.003.

[38] H. H. Phan-Dao, H. Nguyen-Xuan, C. Thai-Hoang, T. Nguyen-Thoi, and T. Rabczuk. An edge-based smoothed finite element method for analysis of laminated composite plates. *International Journal of Computational Methods*, **10**, (01), (2013). doi:10.1142/s0219876213400057.

[39] H. Nguyen-Xuan, G. R. Liu, C. Thai-Hoang, and T. Nguyen-Thoi. An edge-based smoothed finite element method (ES-FEM) with stabilized discrete shear gap technique for analysis of

Reissner–Mindlin plates. *Computer Methods in Applied Mechanics and Engineering*, **199**, (9-12), (2010), pp. 471–489. doi:10.1016/j.cma.2009.09.001.

[40] T. Nguyen-Thoi, T. Bui-Xuan, P. Phung-Van, S. Nguyen-Hoang, and H. Nguyen-Xuan. An edge-based smoothed three-node Mindlin plate element (ES-MIN3) for static and free vibration analyses of plates. *KSCE Journal of Civil Engineering*, **18**, (4), (2014), pp. 1072–1082. doi:10.1007/s12205-014-0002-8.

[41] H. Nguyen-Xuan, T. Rabczuk, N. Nguyen-Thanh, T. Nguyen-Thoi, and S. Bordas. A node-based smoothed finite element method with stabilized discrete shear gap technique for analysis of Reissner–Mindlin plates. *Computational Mechanics*, **46**, (5), (2010), pp. 679–701. doi:10.1007/s00466-010-0509-x.

[42] T. Nguyen-Thoi, T. Bui-Xuan, P. Phung-Van, H. Nguyen-Xuan, and P. Ngo-Thanh. Static, free vibration and buckling analyses of stiffened plates by CS-FEM-DSG3 using triangular elements. *Computers & Structures*, **125**, (2013), pp. 100–113. doi:10.1016/j.compstruc.2013.04.027.

[43] T. Nguyen-Thoi, P. Phung-Van, C. Thai-Hoang, and H. Nguyen-Xuan. A cell-based smoothed discrete shear gap method (CS-DSG3) using triangular elements for static and free vibration analyses of shell structures. *International Journal of Mechanical Sciences*, **74**, (2013), pp. 32–45. doi:10.1016/j.ijmecsci.2013.04.005.

[44] K.-U. Bletzinger, M. Bischoff, and E. Ramm. A unified approach for shear-locking-free triangular and rectangular shell finite elements. *Computers & Structures*, **75**, (3), (2000), pp. 321–334. doi:10.1016/s0045-7949(99)00140-6.

[45] O. C. Zienkiewicz and R. L. Taylor. *The finite element method for solid and structural mechanics*. Butterworth-Heinemann, (2005).

[46] T. Nguyen-Thoi, P. Phung-Van, H. Nguyen-Xuan, and C. Thai-Hoang. A cell-based smoothed discrete shear gap method using triangular elements for static and free vibration analyses of Reissner–Mindlin plates. *International Journal for Numerical Methods in Engineering*, **91**, (7), (2012), pp. 705–741. doi:10.1002/nme.4289.